Thermal signature of plumes in turbulent convection: The skewness of the derivative

Andrew Belmonte* and Albert Libchaber†
Department of Physics, Princeton University, Princeton, New Jersey 08544
(Received 25 September 1995)

We present experimental evidence that, in the hard turbulence regime of Rayleigh-Bénard convection, the temperature fluctuations are produced by buoyancy, despite the presence of a mean horizontal flow at the plates. In a convection cell of aspect ratio 1, we measure the temperature time derivative for Ra from 2×10^7 to 1×10^{11}, which is skewed toward the negative in the region outside the cold thermal boundary layer. This skewness of the derivative indicates the presence of thermal fronts, or plumes, which are detached from the boundary layer by buoyancy. At higher Ra, the skewness of the derivative is reduced, which we relate to the transition to a turbulent Reynolds number in the velocity boundary layer at $\mathrm{Ra}\sim10^9$. We define a time scale using the derivative to characterize these fronts, and find that its minimum value scales as $\mathrm{Ra}^{-2/3}$ over the entire range of Ra in our experiment. [S1063-651X(96)11405-7]

PACS number(s): 47.27.Cn, 47.27.Te

In the study of Rayleigh-Bénard convection at high Rayleigh number (Ra), a turbulent state has been observed in which the thermal boundary layer thickness scales as $\mathrm{Ra}^{-2/7}$ (or, equivalently, the heat flux or Nusselt number $\mathrm{Nu}\sim\mathrm{Ra}^{2/7}$), and a coherent large scale roll circulates in the cell [1,2]. This state is known as hard turbulence. A proposed model for the 2/7 scaling is based on the fact that the thermal boundary layer is subjected to persistent shear by the large scale circulation [3]; this model treats the temperature fluctuations as passive. Further experiments in this direction have artificially enhanced the shear at the boundaries [4], or measured the temperature and velocity length scales with moveable probes near the boundary [5,6]. It remains an open question whether temperature fluctuations in hard turbulence are detached from the thermal layer by their own buoyancy or by the large scale circulation: is the thermal boundary layer thickness determined by buoyancy or by shear? By examining the boundary layer region experimentally, we find that the asymmetry or skewness of the temperature time derivative is characteristic of buoyantly produced fluctuations, which are thermal fronts or plumes.

In the study of turbulence, the time derivative is an appropriate observable for capturing the dynamics of the flow. It is the simplest way of introducing a timelike element into the statistical approach to turbulent phenomena. The statistics of the time derivative are a measure of the rapidity of changes; thus the high frequency portions of the signal, the part most directly related to the coherent structures in the flow, are amplified. For temperature measurements in convection, since the sharpest gradients are those most recently shed from the thermal layer, it is the scales driving the convective motion which are emphasized. In addition, the derivative can be positive or negative, and thus provides a measure of the asymmetry of the signal. This asymmetry is quantified by the skewness, the third moment around the mean normalized by the cube of the rms. One of the most interesting recent developments in the study of turbulence is the measurement of nonzero skewness in the spatial or temporal derivative of scalars [7–10]. This asymmetry is observed far outside the boundary layers, at high enough Reynolds numbers so that it seems to contradict the assumptions of homogeneous and isotropic scalar distribution. In addition, this skewness of the derivative can be attributed to length scales at which viscous effects are negligible [9,10]. One hypothesis attributes the anomalous skewness to the intermittent occurrence of a coherent structure of the velocity boundary layer, called a ramp [8]. The problem of passive scalar mixing in such situations is also being investigated by numerical simulations [11].

In this paper we present measurements of the temperature time derivative made at various distances from the cold upper plate of a gas filled convection cell, for Rayleigh numbers from 2×10^7 to 1×10^{11}, with a Prandtl number of 0.7 [12]. We find that the derivative is not symmetrical: in the region outside the cold boundary layer, the temperature often drops below the mean more rapidly than it returns, skewing the time derivative toward the negative. This represents the passing of a cold thermal front, a buoyant structure originating from the thermal boundary layer. A negative skewness of the derivative is measured out to many times λ_{th} beyond the thermal layer. We also observe changes in the skewness of the derivative for $\mathrm{Ra}>10^{10}$, which when compared with the previously observed transition to high Reynolds number flow in the large scale circulation [6] can be understood as the progressive effects of mixing. Thus our measurements point to another state of turbulent convection beyond hard turbulence, in which the thermal fluctuations are determined by the turbulent velocity boundary layer. This transition would change the stability mechanism of the thermal boundary layer itself, from buoyancy to passive advection, and would probably also change the scaling of the heat flux with Ra. One would also then expect to measure a positive skewness of the derivative outside the cold boundary layer, similar to that observed in passive scalar experiments.

*Author to whom correspondence should be addressed. Presently at Institut Non-Linéaire de Nice, 1361 route des Lucioles, 06560 Valbonne, France.

†Presently at The Rockefeller University, 1230 York Ave, New York, NY 10021. Also at NEC Research Institute, 4 Independence Way, Princeton, NJ 08540.

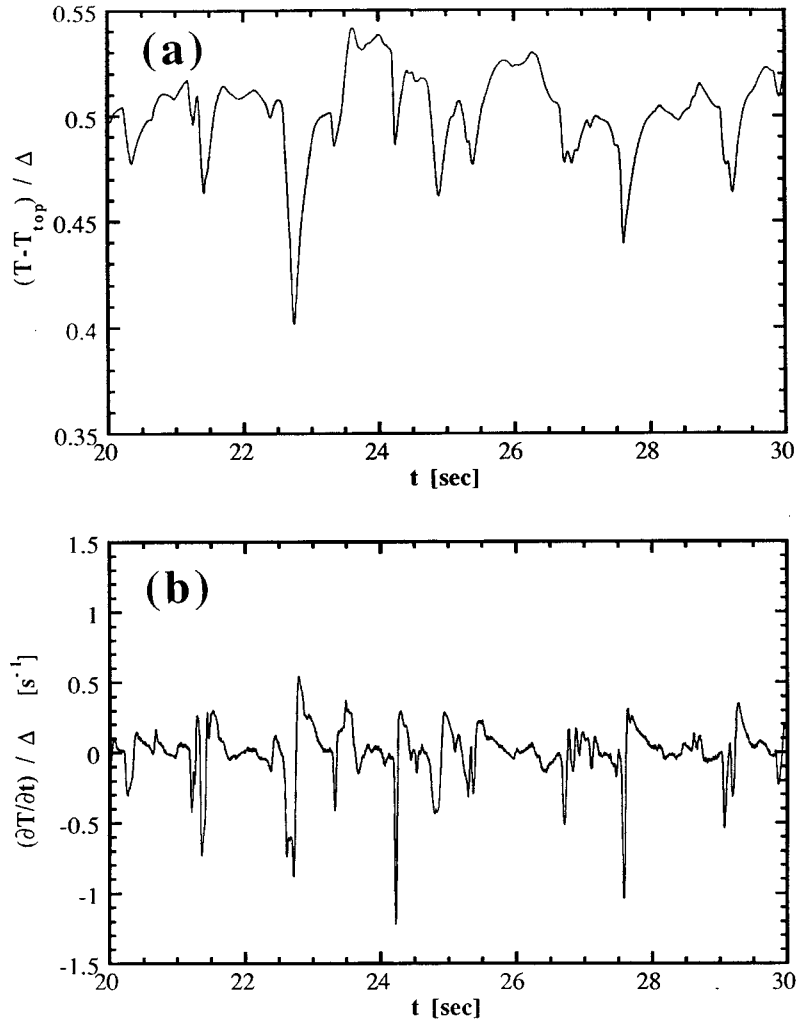

FIG. 1. A temperature time series (a), and its time derivative (b), just outside the thermal boundary layer ($z/\lambda_{th}=5.0$, at λ_m) for $Ra=8.9\times10^8$. T_{top} is the temperature of the top plate, and Δ the temperature difference between the top and bottom plates.

The temperature time series were taken at various distances from the center of the top plate in a cubic convection cell filled with room temperature gas; the experimental setup is described in detail elsewhere [6,12]. The cell has a height L of 15 cm, and is contained within a larger pressure vessel. The control parameter of this experiment, the Rayleigh number Ra [13], is varied over almost six decades by changing the pressure, and by using three different gases (helium, nitrogen, or sulfur hexafluoride). The local temperature in the flow is measured using metal oxide thermistors 200 μm in diameter.

In order to calculate the time derivative $\partial T/\partial t$ from the digitized temperature fluctuations $\{T_i\}$, we compute the average temperature difference

$$dT_i=\frac{(T_{i+1}-T_{i-1})}{2},$$

and divide by the sampling time step Δt, which ranges from 1 to 30 ms. The results are the same if the second nearest neighbors are used instead. This subject was extensively studied for the Chicago helium experiments [14]. We calculate the profiles of the mean, rms, and skewness from the derivative signal at each Ra. The mean is approximately zero in all cases.

In Fig. 1(a) we show temperature fluctuations at $Ra=8.9\times10^8$, taken at a distance of five thermal boundary layer thicknesses (λ_{th}) from the top cold plate. Figure 1(b) is its computed derivative. An asymmetry is visible in the shapes of several of the fluctuations: a rapid initial decrease in temperature, followed by a more gradual increase. The average asymmetry of the derivative is measured by its skewness S', defined as

$$S'\equiv\frac{\left\langle\left(\frac{\partial T}{\partial t}\right)^3\right\rangle}{\left\langle\left(\frac{\partial T}{\partial t}\right)^2\right\rangle^{3/2}}.$$

In Fig. 2 we sketch four possible fluctuations away from the mean, the sign of their contribution to the skewness $S\equiv\langle(T-\langle T\rangle)^3\rangle/\langle(T-\langle T\rangle)^2\rangle^{3/2}$, and to the skewness of the derivative S'. Figure 3 shows the measured profiles $S'(z)$ from our experiment. We find a common shape of $S'(z)$ at each Ra: a broad curve which begins positive inside the cold thermal boundary layer, passes through zero around the edge of the boundary layer, and attains a negative extremum in the region outside. We are unable to find any normalization of the z axis which would collapse the curves of Fig. 3 onto one another, for example by plotting against z/λ_{th}. The region

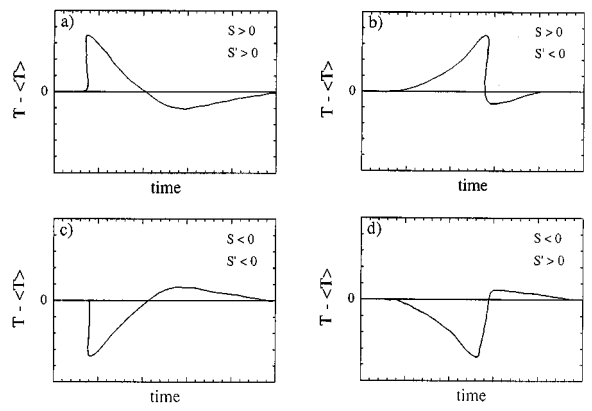

FIG. 2. A sketch of four basic temperature asymmetries relative to the mean $\langle T \rangle$, with the sign of their skewness S, and the skewness of their time derivative S'. Both (a) and (c) correspond to thermal fronts, or plumes, for which $SS' > 0$.

inside the thermal layer, in which $S'(z) > 0$, is due to warmer fluid pulled in from the bulk as colder fluid leaves [6]. Our focus is on this production of cold fluctuations, and on the region outside the thermal layer where $S'(z) < 0$.

In turbulent boundary layer flow experiments where temperature is a passive scalar, thermal fluctuations are produced by instabilities of the velocity layer. In such experiments, $S' > 0$ is measured near a cooled boundary, where most of the fluctuations are toward the cold ($S < 0$); $S' < 0$ is measured near a heated boundary ($S > 0$) [7,9]. The results for a passive scalar are summarized by the relation $SS' < 0$. Our measurements are made near but outside the cold boundary layer, where $S < 0$ [6]; since we measure $S' < 0$, we conclude that the temperature fluctuations are not passively advected. The skewness of the derivative is due to a sharp temperature decrease away from the mean (cooling), followed by a less rapid return (warming): a thermal front. Thus the skewness of the temperature derivative in our experiment is a signature of fluctuations from the boundary layer, which have a form similar to the shape in Fig. 2(c). This temperature profile is characteristic of a plume, thermal, or other object detached from the thermal layer by buoyancy, for which $SS' > 0$ (see Fig. 2). Such objects are clearly observable in visualization studies done in gas [12] and in water [15].

The broadness of the profiles $S'(z)$, which reach an extremum outside the thermal layer (see Fig. 3), imply that the thermal fronts maintain their characteristic shape in this region. This is reminiscent of the mixing zone described in a model for the scaling of hard turbulence [16]. The rms of the temperature derivative, $\theta'(z)$, follows the same shape as the rms of the fluctuations, $\theta(z)$, with a maximum value at the

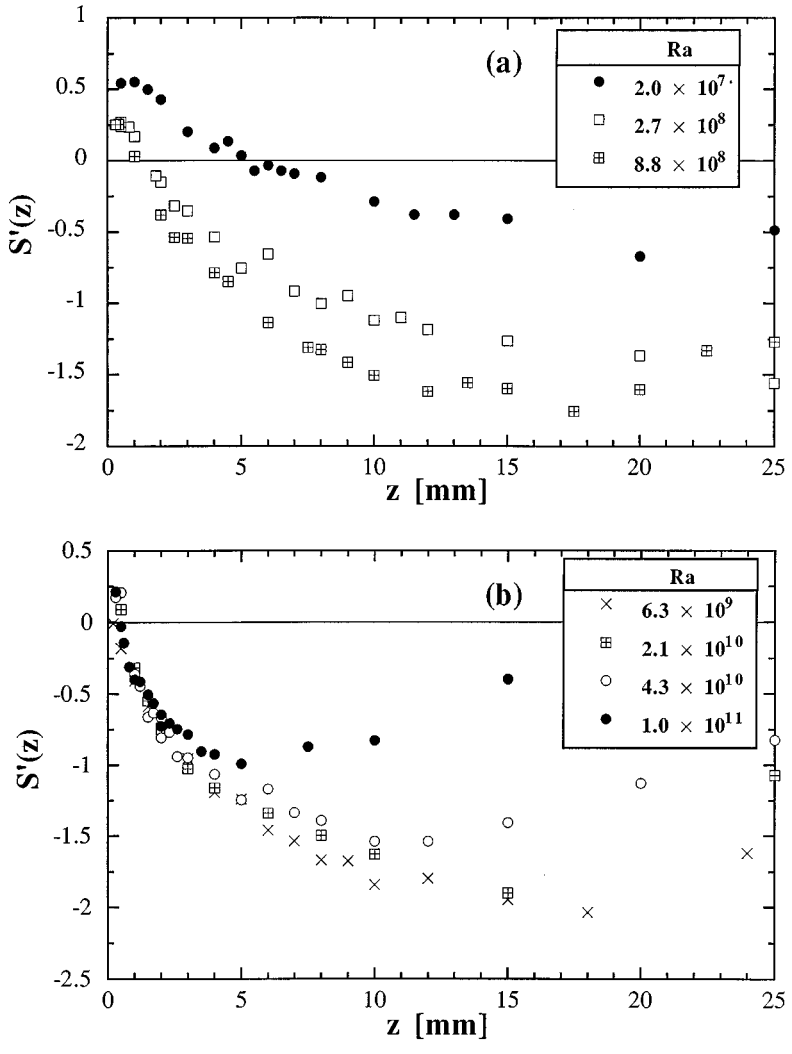

FIG. 3. The skewness of the temperature derivative vs distance from the top plate z for (a) $\mathrm{Ra} = 2.0 \times 10^7$ (black circles), 2.7×10^8 (white squares), and 8.8×10^8 (crossed squares). (b) $\mathrm{Ra} = 6.3 \times 10^9$ (crosses), 2.1×10^{10} (crossed squares), 4.3×10^{10} (white circles), and 1.0×10^{11} (black circles).

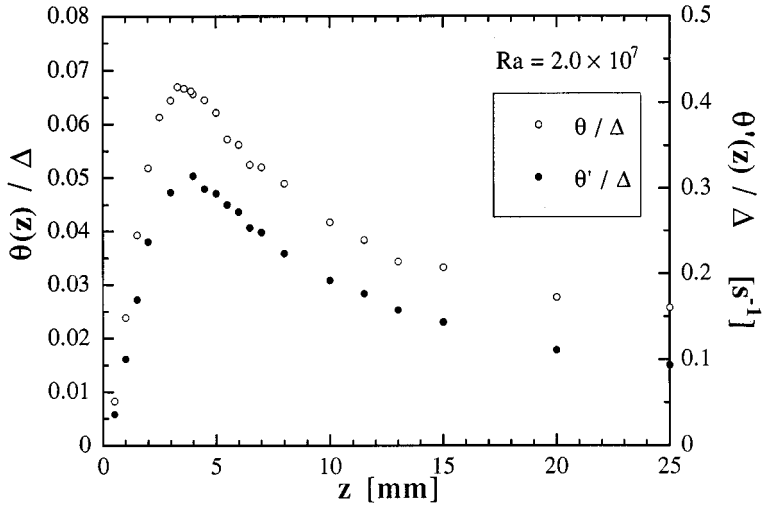

FIG. 4. Profiles of the temperature rms (θ), and the rms of the derivative (θ') for Ra$=2\times10^7$.

edge of the thermal boundary layer [6]; an example is shown in Fig. 4. This similarity is discussed below. Thus the strongest derivatives are located at the thermal layer, indicating that it is still the dominant dynamical structure [17].

We turn next to the changes in the skewness of the derivative as Ra is increased. From 10^7 to about 10^9, the asymmetry represented by $S'(z)$ becomes more pronounced with increasing Ra [Fig. 3(a)]. At higher Ra [Fig. 3(b)], the profiles do not change much within the first few mm of the plate, but the outer part of $S'(z)$ begins to decrease at Ra$\sim10^{10}$. At Ra$=1\times10^{11}$, the overall magnitude of S' is markedly reduced, and its extremum is much closer to the plate. The extremum of the skewness of the derivative, $S'_{\rm EXTR}$, is shown as a function of Ra in Fig. 5. Its magnitude is of order 1, the same size as found in experiments and simulations on passive scalars [7,9–11]. The position of $S'_{\rm EXTR}$ occurs somewhere above 15 mm for Ra$<2\times10^{10}$, though this is not well resolved by our experiment. We plot its approximate location as a function of Ra in Fig. 6, along with the thermal boundary layer thickness $\lambda_{\rm th}$.

In a previous paper [6], we measured the cutoff frequency of the temperature power spectrum, which had a maximum value at some distance λ_m from the plate; the dependence of this distance on Ra is also shown in Fig. 6. We claimed that this is the position of the maximum mean velocity in the large scale circulation. At the onset of hard turbulence, the Reynolds number of the flow along the plate $\mathrm{Re}_m \equiv U\lambda_m/\nu$ is about 50, where U is the velocity of the large scale circulation [1,2]. As Ra increases, λ_m remains constant. For Ra$>2\times10^9$, λ_m begins to decrease with Ra, such that Re_m has a constant value of about 600, a typical size for a turbulent boundary layer. Thus there is a turbulent transition in the large scale circulation at Ra$\sim10^9$. The thickness of the thermal layer $\lambda_{\rm th}$ is far from λ_m at the onset of this transition, so the 2/7 scaling of $\lambda_{\rm th}$ is unaffected. However, an extrapolation of the two trends in Fig. 6 shows that λ_m will cross $\lambda_{\rm th}$ for Ra$\gtrsim10^{14}$, which could give rise to a new scaling regime [6]. In the present experiment, as λ_m approaches $\lambda_{\rm th}$, the reduction observed in $S'_{\rm EXTR}$ for Ra$>10^{10}$ (Fig. 5) could be due to an enhanced mixing of the plumes. Ultimately, as Ra increases and the flow along the plate becomes the dominant mechanism for creating temperature fluctuations, we expect $S'_{\rm EXTR}$ to become positive.

Thinking along these lines we are led to reconsider the transition to hard turbulence at Ra$=10^7$. At this stage the Reynolds number of the *whole cell*, $\mathrm{Re}_L \equiv UL/\nu$, is at a transitional value of about 1000 [1,2]. The onset of hard turbulence could therefore be caused by a sufficient mixing in the

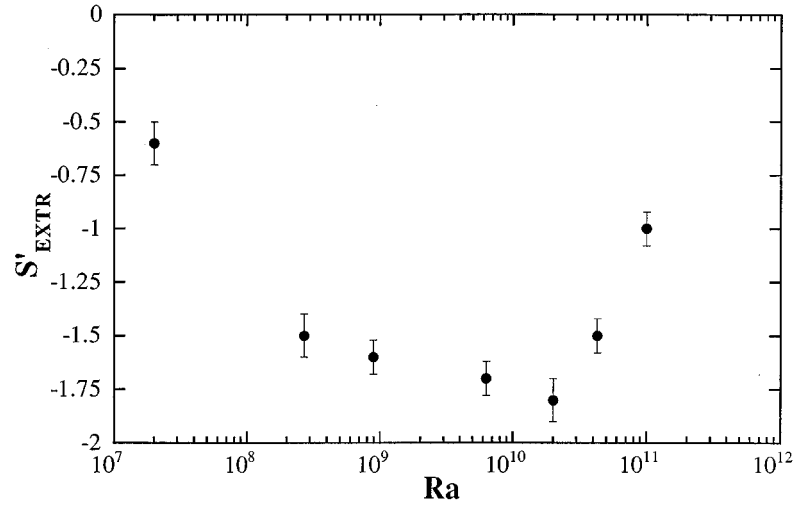

FIG. 5. The extremum of the skewness of the derivative $S'_{\rm EXTR}$ vs Ra.

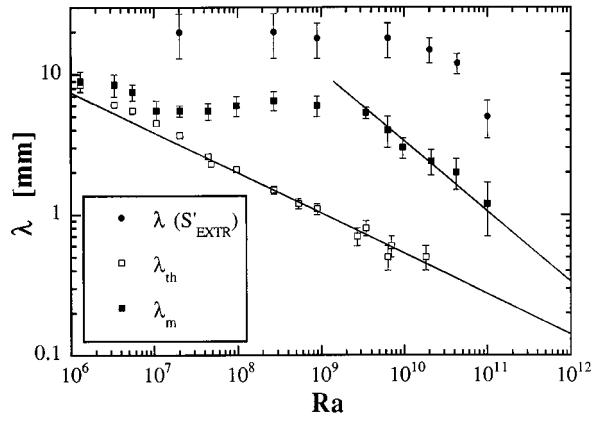

FIG. 6. The positions of the extremum of the skewness of the derivative (black circles) vs Ra. Included in the plot are the thermal boundary layer thickness λ_{th} (white squares), and the position of the maximum cutoff frequency λ_m (black squares) from Ref. [6]. The lines drawn for λ_{th} and λ_m corresponds to $\mathrm{Ra}^{-2/7}$ and $\mathrm{Ra}^{-1/2}$, respectively.

cell such that the effective eddy viscosity restabilizes a coherent large scale circulation, similar to that observed just beyond the onset of convection [18]. The interplay between the large Reynolds number turbulence of the large scale circulation and the turbulence due to buoyant plumes seems an essential aspect of hard turbulence.

We can define a thermal time scale τ_θ using the time derivative by taking the ratio of the rms of the fluctuations to the rms of the derivative:

$$\tau_\theta \equiv \frac{\langle (T-\langle T\rangle)^2\rangle^{1/2}}{\left\langle \left(\frac{\partial T}{\partial t}\right)^2\right\rangle^{1/2}};$$

this is a sort of thermal Taylor microtime [19], characterizing the dynamics of the temperature fluctuations. An example of the dependence of τ_θ on height is shown in Fig. 7; the fact that $\tau_\theta(z)$ is not strongly dependent on z is a reflection of the similarity of $\theta(z)$ and $\theta'(z)$, shown in Fig. 4. The time scale has a minimum value $\tau_{\theta\,\mathrm{MIN}}\sim 0.21$ s, in a rather broad region

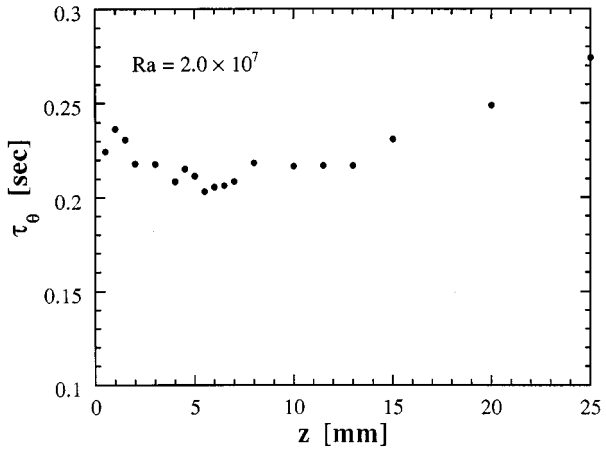

FIG. 7. Profile of the thermal timescale τ_θ (defined in the text) vs height z for $\mathrm{Ra}=2\times10^7$.

in the vicinity of the thermal boundary layer, due to the sharp gradients (i.e., the coherent structures) in this region. In Fig. 8 we plot $\tau_{\theta\,\mathrm{MIN}}$ at each Ra, made dimensionless by the thermal diffusion time for the cell L^2/κ, where κ is the thermal diffusivity, and L the cell height; the brackets in Fig. 8 show the full extent of the variation of τ_θ for z from 0 to 25 mm. This dimensionless time is in fact the inverse of a quantity defined by Procaccia *et al.* [20], which they called the dissipative power:

$$Q=\frac{L^2}{\kappa}\frac{1}{\tau_\theta}.$$

From Fig. 8 we find that $\tau_{\theta\,\mathrm{MIN}}$ scales with Ra as

$$\frac{\tau_{\theta\,\mathrm{MIN}}\kappa}{L^2}\sim \mathrm{Ra}^{-0.68\pm0.03}.$$

This is in excellent agreement with the scaling $Q\sim\mathrm{Ra}^{0.67\pm0.04}$ measured in low temperature helium gas for $\mathrm{Ra}<10^{11}$ [2,20]. We observe no change in the scaling of $\tau_{\theta\,\mathrm{MIN}}$ at $\mathrm{Ra}\sim10^{10}$, where the skewness of the derivative decreases. Thus for $10^7<\mathrm{Ra}<10^{11}$, $\tau_{\theta\,\mathrm{MIN}}\sim\mathrm{Ra}^{-2/3}$.

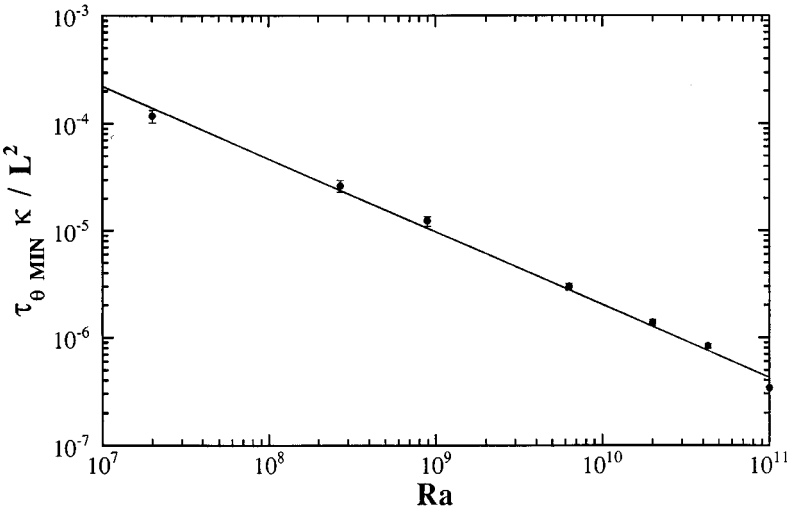

FIG. 8. The minimum thermal time scale $\tau_{\theta\,\mathrm{MIN}}$, normalized by the diffusion time L^2/κ, vs Ra. The line corresponds to the fitted scaling $\mathrm{Ra}^{-0.68}$. The brackets indicate the entire variation of $\tau_\theta(z)$ in the range $0<z<25$ mm.

In conclusion, we have studied the coherent structures of thermal fluctuations in hard turbulence through the skewness of the time derivative. A typical such structure is the thermal plume, a buoyant mushroom of hot or cold fluid which erupts from the thermal boundary layer, carrying heat; thus they contribute to the total heat flux through the cell. In hard turbulence the plumes depart under conditions of shear, and begin their vertical climb or descent in the horizontal wind of the large scale circulation. It could very well be that the entire character of hard turbulence is determined by this interaction of buoyant plume and mean flow. In this paper we have only begun to study the signature of these plumes. The problem deserves further study.

Although we have not addressed the question of intermittency in this paper, a similar approach could be taken, using the fourth moment of the fluctuations. As two, three, and higher point correlations become increasingly important in the study of turbulence, it would be particularly interesting to compare such measurements for the case of a buoyant (active) scalar, as discussed here, with results from passive scalar experiments and numerical simulations.

The asymptotic state of turbulent Rayleigh-Bénard convection ($\mathrm{Ra}\to\infty$) has often been a subject of theoretical speculation [21]. Experimentally, hard turbulence is an organized state of convection which begins at $\mathrm{Ra}\sim10^7$, and extends at least seven orders of magnitude in Ra [1,2], up to the present experimental limit. Is hard turbulence asymptotic? From our point of view, there is a progressive series of changes beginning at $\mathrm{Ra}\sim10^9$, which are connected to the $\mathrm{Re}_m\sim1000$ transition in the large scale circulation. It is worth recalling that none of these changes affected the 2/7 scaling of the heat flux or the other gross characteristics of hard turbulence. They may, however, be the precursors of a new state, which will appear beyond hard turbulence. What these experiments show is that the temperature fluctuations outside the boundary layer are affected by the large scale circulation as it becomes more turbulent, and it is reasonable to expect the thermal boundary layer itself to be affected eventually. The next state of turbulent convection remains to be discovered.

We thank B. Shraiman and E. Siggia for many fruitful discussions, and for providing us with the suggestion to measure the skewness of the derivative in the first place. We also thank J.-M. Flesselles, Ning Li, A. Pumir, and V. Yakhot for enlightening discussions.

[1] F. Heslot, B. Castaing, and A. Libchaber, Phys. Rev. A **36**, 5870 (1987); M. Sano, X. Z. Wu, and A. Libchaber, *ibid*. **40**, 6421 (1989); X. Z. Wu and A. Libchaber, *ibid*. **45**, 842 (1992).

[2] X. Z. Wu, Ph.D. thesis, University of Chicago, 1991 (unpublished).

[3] B. Shraiman and E. Siggia, Phys. Rev. A **42**, 3650 (1990); see also E. Siggia, Ann. Rev. Fluid Mech. **26**, 137 (1994).

[4] T. Solomon and J. Gollub, Phys. Rev. Lett. **64**, 2382 (1990); Phys. Rev. A **43**, 6683 (1991).

[5] A. Tilgner, A. Belmonte, and A. Libchaber, Phys. Rev. E **47**, 2253 (1993).

[6] A. Belmonte, A. Tilgner, and A. Libchaber, Phys. Rev. E **50**, 269 (1994).

[7] K. Sreenivasan, R. Antonia, and H. Danh, Phys. Fluids **20**, 1238 (1977); K. Sreenivasan and S. Tavoularis, J. Fluid Mech. **101**, 783 (1980); S. Thoroddsen and C. Van Atta, *ibid*. **244**, 547 (1992); C. Tong and Z. Warhaft, Phys. Fluids **6**, 2165 (1994).

[8] K. Sreenivasan and R. Antonia, Phys. Fluids **20**, 1986 (1977); R. Antonia and C. Van Atta, *ibid*. **22**, 2430 (1979).

[9] P. Mestayer, J. Fluid Mech. **125**, 475 (1982).

[10] K. Sreenivasan, Proc. R. Soc. London Ser. A **434**, 165 (1991).

[11] M. Holzer and E. D. Siggia, Phys. Fluids **6**, 1820 (1994); A. Pumir, *ibid*. **6**, 2118 (1994).

[12] A. Belmonte, Ph.D. thesis, Princeton University, 1994 (unpublished).

[13] The Rayleigh number is defined as $\mathrm{Ra}=g\alpha\Delta L^3/\nu\kappa$, where g is the gravitational acceleration, L the height of the cell, Δ the temperature difference, α the thermal expansion coefficient of the fluid, ν its kinematic viscosity, and κ its thermal diffusivity. The Prandtl number is the ratio of the two diffusion constants: $Pr=\nu/\kappa$.

[14] This means that we are indeed within the limit where $dT_i/\Delta t\sim\partial T/\partial t$, see E. S. C. Ching, Phys. Rev. A **44**, 3622 (1991); also see E. S. C. Ching, L. Kadanoff, A. Libchaber, and X. Z. Wu, Physica D **58**, 414 (1992).

[15] G. Zocchi, E. Moses, and A. Libchaber, Physica A **166**, 387 (1990); E. Moses, G. Zocchi, and A. Libchaber, J. Fluid Mech. **251**, 581 (1993).

[16] B. Castaing, G. Gunaratne, F. Heslot, L. Kadanoff, A. Libchaber, S. Thomae, X. Z. Wu, S. Zaleski, and G. Zanetti, J. Fluid Mech. **204**, 1 (1989).

[17] There are some indications that the maximum of $\theta'(z)$ occurs outside of λ_{th} at higher Ra, but our spatial resolution does not allow us to state this with certainty.

[18] S. Chandrasekhar, *Hydrodynamic and Hydromagnetic Stability* (Clarendon, Oxford, 1961).

[19] H. Tennekes and J. L. Lumley, *A First Course in Turbulence* (MIT Press, Cambridge, MA, 1972).

[20] I. Procaccia, E. S. C. Ching, P. Constantin, L. Kadanoff, A. Libchaber, and X. Z. Wu, Phys. Rev. A **44**, 8091 (1991).

[21] W. V. R. Malkus, Proc. R. Soc. London Ser. A **225**, 196 (1954); R. Kraichnan, Phys. Fluids **5**, 1374 (1962); L. Howard, J. Fluid Mech. **17**, 405 (1963); F. Busse, *ibid*. **37**, 457 (1969); L. Howard, Studies Appl. Math. **83**, 273 (1990).